

DOI:

# Design of Inlet Distortion Generators for Direct-Connect Scramjet Combustors

Enrico Degregori\*<sup>†</sup> and Michele Ferlauto\*

\* *Mechanical and Aerospace Engineering Department, Politecnico di Torino  
corso Duca degli Abruzzi, 24, 10129 Turin, Italy*

enrico.degregori@studenti.polito.it · michele.ferlauto@polito.it

<sup>†</sup> Corresponding Author

## Abstract

The paper deals with the design of an aerodynamic device that acts as a facility nozzle and as inlet distortion generator in a direct-connect scramjet combustor test-rig. The device does not only replicate a reference in-flight condition, but also it is also supposed to replicate the dynamic response of the system close to the operating point. This consideration leads to the choice of the inlet cowl section as the reference section for the facility nozzle design. The solution of the design problem is sought by using different approaches of CFD analysis and optimization tools. Numerical simulations based on methods ranging from the method of characteristics to the RANS equations are concerned. The initial design is based on the solution of an inverse problem coupled to optimization by genetic algorithms. The candidate solution are then tested by CFD simulations of the direct-connect facility and the resulting shock reflection patterns are compared to the corresponding patterns computed at the in-flight configurations. The reliability of the design is then evaluated by numerical simulations of the flowfield of the whole direct-connect facility by using a flow solver of the compressible RANS equations. The proposed procedure is checked by designing a nozzle-distortion generator system for a scramjet combustor test-rig model available in the open literature.

## Introduction

Because of the severe limitations imposed by the supersonic combustion in hypersonic air-breathing propulsion systems the coupling between hypersonic isolator and combustor is extensively studied both by CFD and experimental investigations.<sup>1-5</sup> The latter approach is somehow privileged. Experimental testings on scramjet combustor are generally carried out in direct-connect scramjet (DCS) test-rigs (nozzle + isolator + combustor). This configuration offers substantial advantages in terms of experimental costs, test duration, and experimental complexity with respect to the free-jet facility (e.g. inlet + isolator + combustor). Moreover, large-scale scramjets can only be investigated through direct-connect experiments.<sup>1</sup> In the traditional DCS test-rigs, a Facility Nozzle (FN) is placed before the isolator-combustor system that simulates the scramjet. The nozzle generates a nearly uniform flow at the prescribed inlet Mach number but this strategy does not simulate the actual situation. Actually, the flow is highly distorted by the oblique shocks generated by the scramjet inlet and by the boundary layer that develops on the long inlet surface.<sup>6</sup> Since the combustor is among the most crucial components in scramjet engines, these flow distortions must be reproduced accurately in order to verify the engine performances in real working conditions. This scenario raises concerns on the design approach to the direct-connect facility and on its ability in simulating the flight environment and operability. New design approaches have been therefore proposed, supported by the wide use of CFD for determining the aerodynamic effects of distortion devices such as ramps, injection slots and ports.<sup>4,7</sup> It has been shown that the combined application of injection slots and ports can effectively mimic the distortion flow generated by the scramjet inlet.<sup>4</sup> In Ref. 7 a ramp is used to generate shocks and to mimic flow distortion. In such configuration, facility nozzles with large contraction ratios may unstart the direct-connect facility. Other design solutions does not suffer of unstart problems.<sup>8</sup> Often the strongest shocks are not replicated by the test facility and the experimental testing starts from a secondary or tertiary shock reflection. This design choice is economically advantageous when a single, steady-state working condition is of interest, but it precludes any accurate investigation of the inlet-isolator-combustor dynamics. The latter is essential for understanding the integrated system stability with respect to unsteadiness and, eventually, to dual-mode switching (ramjet/scramjet) procedures. In order to include these features, the supersonic flow must be replicated starting from

## DESIGN OF INLET DISTORTION GENERATORS FOR SCRAMJET

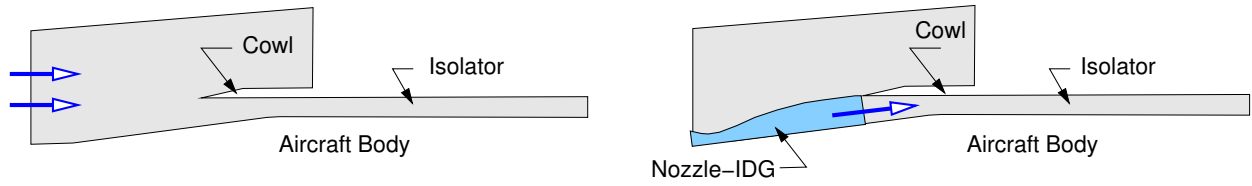


Figure 1: Sketch of the free-stream configuration and of the direct-connect facility model.

the cowl-lip section, where the oblique shock is generated by geometrical reasons. In fact, the location of any further shock reflection may vary according to the combustor working conditions.

Aim of the present study is to design the facility nozzle system for the direct-connect test-rig and to analyze and assess the solution obtained in a multi-point design perspective. The key point is to establish how accurately a fixed geometry Facility Nozzle/Inlet Distortion Generator (FN-IDG) assembly, attached to the direct connect test-rig, can replicate the unsteady evolution of the shock trains in the scramjet. This analysis is carried out by using both low order models and fully unsteady RANS simulations. The facility nozzle and the inlet distortion generator are considered as an integrated device and designed from scratch by using inverse methods and optimization techniques based on genetic algorithms. The simplified geometry of scramjet facility proposed in Ref. 8 has been used as a reference. By using a fast marching inverse technique based on the Method of Characteristics (MoC), several facility nozzles working at different Mach numbers has been designed and tested. the CFD solution of the shock structures and shock reflections generated by the direct-connect facility are compared to that generated in-flight. Finally the fully turbulent RANS solution of the whole direct connect facility is studied.

## Mathematical Model

The aerodynamic design problem can be solved by using many different approaches, as for instance, the shape optimization by using gradient based or stochastic method<sup>9,10</sup> or by reformulating the design as an inverse problem.<sup>8,11,12</sup> The latter approach is used here, by coupling an inverse method with an evolutionary optimizer based on Genetic Algorithms (GA).<sup>10</sup> It is well known that such GA require a large number of iteration to converge. Therefore the solution of the inverse problem should rely on a fast computational approach, as for instance, the Method of Characteristics (MoC). In the following section we outline the mathematical models used throughout our numerical study.

### Method of Characteristics

The method of characteristics is resumed here for steady two-dimensional supersonic flows. The starting point are the Euler equations written in the quasi-linear form

$$\begin{aligned} \rho u_x + \rho v_y + u\rho_x + v\rho_y + \delta\rho v/y &= 0 \\ \rho uu_x + \rho vv_y + p_x &= 0 \\ \rho uv_x + \rho vv_y + p_y &= 0 \\ up_x + vp_y - a^2\rho_x - a^2v\rho_y &= 0 \end{aligned} \quad (1)$$

As usual,  $\rho$ ,  $p$ ,  $a$  are density, pressure and speed of sound, respectively;  $u$ ,  $v$  are the flow velocity cartesian components.  $\delta = 0$  holds for planar flow and  $\delta = 1$  for axisymmetric flow.

The MoC transforms the PDE system (1) in the following ODE system

$$\rho V dV + dp = 0 \quad (2)$$

$$dp - a^2 d\rho = 0 \quad (3)$$

$$\frac{\sqrt{M^2 - 1}}{\rho V^2} dp_{\pm} \pm d\theta_{\pm} + \delta \left[ \frac{\sin \theta dx_{\pm}}{yM \cos(\theta \pm \alpha)} \right] = 0 \quad (4)$$

along the characteristic lines

$$\left( \frac{dy}{dx} \right)_o = \lambda_o = \frac{v}{u} \quad \left( \frac{dy}{dx} \right)_{\pm} = \lambda_{\pm} = \tan(\theta \pm \alpha) \quad (5)$$

where  $\theta = \arctan(v/u)$  is the flow angle and  $\alpha = \arctan(1/M)$ .

In a rotational flow three characteristics pass through each point of the field: the streamline and two Mach lines. Consequently, the system of ordinary differential equations is composed of two compatibility equations along

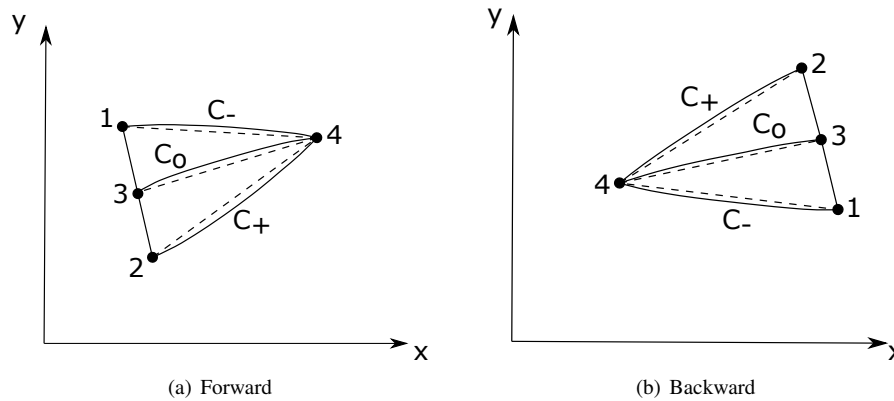


Figure 2: Method of Characteristics. Backward and forward projection of the wave signals.

the streamline and two equations along the Mach lines. In the present analysis, a finite difference network is built for the marching method based on the Mach lines. The numerical method employed is the Euler predictor-corrector based on the average property method. This is a second order method for integrating ordinary differential equations.<sup>13</sup> We used the MoC for solving the inverse problem of deriving the facility nozzle shape from the knowledge of the pressure distribution on the nozzle upper-wall and the flow solution along a certain region of the flowfield.

### Inverse Design using forward MoC

A first method of solving the inverse problem is based on projecting the characteristics forward. In this case, the initial value line is the sonic line of the nozzle, which is approximated with a second order polynomial. The interior point is evaluated through the intersection of two Mach lines ( $C_+$  and  $C_-$ ) starting from the initial points 1 and 2 and then the streamline ( $C_o$ ) is used to find point 3, as shown in Figure 2(a). The pressure distribution, represented through a third order polynomial.

$$p(x) = a_0 + a_1x + a_2x^2 + a_3x^3 \quad (6)$$

in imposed as boundary condition on the upper wall. On the lower boundary condition we imposed the flow direction. A genetic algorithm code is used to optimize the shape of the nozzle, by using the polynomial coefficients as controls. The objective function is defined as

$$J = \frac{K_1}{\sqrt{\frac{\sum_i (M_i - M_{ref})^2 \Delta y_i}{\sum_i \Delta y_i}}} + \frac{K_2}{\sqrt{\frac{\sum_i \theta_i^2 \Delta y_i}{\sum_i \Delta y_i}}} + \frac{K_3}{(h - h_{ex})^2} \quad (7)$$

in order to satisfy the geometric constraints of the experimental facility and to have the prescribed distribution of the Mach at the exit section. The coefficients  $K_1$ ,  $K_2$  and  $K_3$  are weights of the functional  $J$ . The code changes the pressure distribution using the genetic algorithm in order to maximize this function. In particular, the coefficients  $a_0$  and  $a_1$  are defined by the imposed pressure at the throat and at the exit section, thus there are two degrees of freedom, that is, the coefficient  $a_2$  and the inflection point  $x_f$ , which also depends on the coefficient  $a_3$ .

### Inverse Design using backward MoC

Another design method projects the characteristics backward. In this case, the flow feature are prescribed at the nozzle exit. The procedure and the boundary conditions are analogous to the forward method, indeed the solution point is evaluated through the intersection of two Mach lines and then the streamline is used to find point 3 (see Figure 2(b)). The solver stops when the sonic line of the nozzle is reached, the objective is to find a pressure distribution that allows to reach the sonic line.

$$J = \frac{1}{\frac{\sum_i^N (M_i - 1)}{N}} \quad (8)$$

The genetic algorithm maximizes this function changing the pressure distribution, in this way the sonic line is reached with a certain degree of tolerance.

## DESIGN OF INLET DISTORTION GENERATORS FOR SCRAMJET

**Flow Governing Equations**

The main flow is governed by the compressible Unsteady Reynolds Averaged Navier-Stokes equations (URANS). The one-equation model of Spalart-Allmaras (S-A)<sup>14,15</sup> is used for the turbulence modelling. The set of governing equations are written in the compact integral form

$$\frac{\partial}{\partial t} \int_{\mathcal{V}} \vec{W} d\mathcal{V} + \int_{\mathcal{S}} \vec{F}_I \cdot \hat{n} d\mathcal{S} + \int_{\mathcal{S}} \vec{F}_V \cdot \hat{n} d\mathcal{S} = \int_{\mathcal{V}} \vec{H} d\mathcal{V} \quad (9)$$

where  $\mathcal{V}$  represents an arbitrary volume enclosed in a surface  $\mathcal{S}$ .  $\vec{W}$  is the hyper-vector of conservative variables,  $\vec{F}_I$  and  $\vec{F}_V$  are tensors containing the inviscid and the viscous fluxes, respectively, and  $\vec{H}$  is a non-homogeneous term defined as follows

$$\begin{aligned} \vec{W} &= \{\rho, \rho \vec{q}, E, \tilde{v}_t\}^T \\ \vec{F}_I &= \{\rho \vec{q}, p \bar{I} + \rho \vec{q} \otimes \vec{q}, (E + p) \vec{q}, \tilde{v}_t \vec{q}\}^T \\ \vec{F}_V &= \frac{\sqrt{\gamma M_\infty}}{\text{Re}_\infty} \left\{ 0, -\bar{\tau}, -\kappa \nabla T - \bar{\tau} \cdot \vec{q}, -\frac{\nu + \tilde{v}_t}{\sigma} \nabla \tilde{v}_t \right\}^T \\ \vec{H} &= \{0, 0, 0, Q(\tilde{v}_t)\}^T \end{aligned} \quad (10)$$

$\vec{q} = \{u, v, w\}^T$  is the velocity vector,  $E$  the total energy per unit volume,  $M_\infty$  and  $\text{Re}_\infty$  are the free-stream Mach number and the Reynolds number,  $\gamma$  is the ratio of the specific heats and finally  $\bar{I}$  is the unit matrix. The non-homogeneous term  $\vec{H}$  contains a non-null component  $Q(\tilde{v}_t)$  only. The definition and role of  $Q$  in the turbulence model is addressed in the next paragraphs.

System (9) is reduced to non-dimensional form with respect to the following reference values:  $L$  for length,  $\rho_\infty$  for density,  $T_\infty$  for temperature,  $\sqrt{RT_\infty}$  for velocity,  $RT_\infty$  for energy per unit mass and  $\mu_\infty$  for viscosity. The viscous stresses are written as

$$\tau_{ij} = (\mu + \mu_t) \left[ \frac{\partial q_j}{\partial x_i} + \frac{\partial q_i}{\partial x_j} - \frac{2}{3} (\nabla \cdot \vec{q}) \delta_{ij} \right] \quad (11)$$

The thermal conductivity  $\kappa$  is calculated in nondimensional form as

$$\kappa = \frac{\gamma}{\gamma - 1} \left( \frac{\mu}{Pr} + \frac{\mu_t}{Pr_t} \right) \quad (12)$$

where  $Pr$  and  $Pr_t$  are the laminar and turbulent Prandtl numbers. The laminar viscosity  $\mu$  is calculated by the Sutherland's law

$$\mu(T) = T^{3/2} \left( \frac{1 + T_{\text{ref}}}{T + T_{\text{ref}}} \right) \quad T_{\text{ref}} = \frac{110.4}{T_\infty} \quad (13)$$

The turbulent viscosity  $\mu_t = \rho \nu_t$  is computed through the Spalart-Allmaras one-equation model.<sup>14</sup> Finally, the perfect gas relationship  $p = \rho T$  completes the set of equations. The numerical solution of system (9) is based on a shock capturing Godunov method using flux-difference splitting techniques and a second order accurate Essentially Non-Oscillatory (ENO) scheme.<sup>16</sup> The integration in time is carried out according to a 4th order Runge Kutta scheme. The numerical method has been efficiently parallelized by using OpenMP directives. The spatial and time accuracy of the flow solver has been widely tested in many unsteady compressible flowfield such as, for instance, the flow manipulation by synthetic jets and the post-stall control of NACA0015 profile;<sup>17</sup> in time-dependent flows with moving grids;<sup>18</sup> in the study of unsteady reacting flows.<sup>19</sup>

In the Godunov methods<sup>20</sup> the solution is advanced in time and space by computing the numerical fluxes at each cell interface. The convective fluxes  $F_I$  are evaluated by solving a Riemann's problem at each cell interfaces. The left and right states of the Riemann problem are computed according to the reconstruction phase of the ENO scheme. If a first order reconstruction scheme is adopted, the generic conservative variable  $U$  is assumed as an averaged, constant value inside each cell (Fig. 3, right up). Second order accuracy is achieved by assuming a linear, instead of constant, behavior of the conservative variable  $U$  inside the cells. The solution of the Riemann problem describes how the collapse of such a discontinuity generates a pattern of waves along which signals propagate in time. Convective fluxes  $F_I$  are then computed according to a flux-difference splitting approach.<sup>21</sup> The computation of the viscous fluxes  $F_V$  requires the evaluation of the velocity and temperature gradients at the cell interfaces by using an integral technique and the Gauss Theorem<sup>18</sup>. The same approach is used when computing the gradient of turbulent quantities. The Boundary Condition (BC) enforcement follows the guidelines of the characteristic based approach.<sup>18,22</sup>

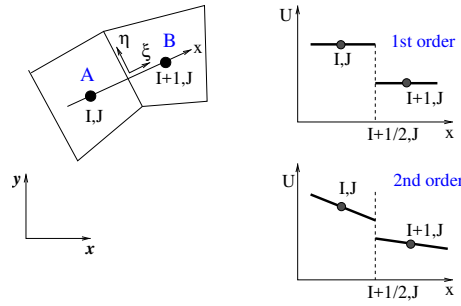


Figure 3: Riemann problem.

The Spalart-Allmaras turbulence model expresses the evolution equation of the *modified eddy viscosity*  $\tilde{\nu}_t$ . The eddy viscosity  $\mu_t$ , or turbulent viscosity, needed in the viscous stress tensor (11) is obtained from  $\tilde{\nu}_t$  as

$$\mu_t = \rho \tilde{\nu}_t f_{v1}, \quad f_{v1} = \frac{\chi^3}{\chi^3 + c_{v1}^3}, \quad \chi \equiv \frac{\tilde{\nu}_t}{\nu} \quad (14)$$

The variable  $\tilde{\nu}_t$  is solved by the last equation of the system (9). This equation, hereafter called the *turbulence equation*, is basically of similar form to the equations for basic flow variable such as mass, momentum and total energy. The turbulence equation contains a complex source term  $Q$  inside the vector  $\vec{H}$ . The basic source term without transition terms is

$$Q = c_{b1} \tilde{S} \tilde{\nu}_t - \frac{\sqrt{\gamma} M_\infty}{\text{Re}_\infty} \left[ c_{w1} f_w \left( \frac{\tilde{\nu}_t}{d} \right)^2 + \frac{c_{b2}}{\sigma} (\nabla \tilde{\nu}_t)^2 \right] \quad (15)$$

where the first term represents production and the second term represents destruction of  $\tilde{\nu}$ . The third term is called the first-order diffusion term. In the production term, the modified magnitude  $\tilde{S}$  of vorticity is introduced

$$\tilde{S} = S + \frac{\sqrt{\gamma} M_\infty}{\text{Re}_\infty} \frac{\tilde{\nu}}{\kappa^2 d^2} f_{v2}, \quad f_{v2} = 1 - \frac{\chi}{1 + \chi f_{v1}} \quad (16)$$

where  $S = \left| \frac{\partial v}{\partial x} - \frac{\partial u}{\partial y} \right|$  is the magnitude of vorticity and  $d$  is the distance to the nearest wall. In the destruction term, the function  $f_w$  is defined as

$$f_w = g \left[ \frac{1 + c_{w3}}{g^6 + c_{w3}^6} \right]^{\frac{1}{6}} \quad g = r + c_{w2}(r^6 - r), \quad r = \frac{\sqrt{\gamma} M_\infty}{\text{Re}_\infty} \frac{\tilde{\nu}}{\tilde{S} \kappa^2 d^2} \quad (17)$$

The constants are set as  $c_{b1} = 0.1355$ ,  $c_{b2} = 0.622$ ,  $\sigma = 2/3$ ,  $\kappa = 0.41$ ,  $c_{w1} = c_{b1}/\kappa^2 + (1 + c_{b2})/\sigma$ ,  $c_{w2} = 0.3$ ,  $c_{w3} = 2$ ,  $c_{v1} = 7.1$ . Concerning the boundary conditions, a free-stream eddy viscosity  $\tilde{\nu}_{t\infty}$  is specified by setting a value for at the free-stream boundaries. Usually it can be set to zero. The eddy viscosity is also set to zero on the wall surfaces.

## Numerical Results

The reference test-case adopted is scramjet combustor model proposed by Yu et al.<sup>8</sup> and it simulates the flowpath of a simple configuration of inlet and isolator. The inlet is designed for a shock-on-lip Mach number of 4.0 over a single inlet ramp that is inclined by 7 degrees. The ramp is 314.5 mm long, and the contraction ratio of the internal area of the inlet is 1.44. A constant cross-sectional isolator (350 mm long and 30 mm high) is built beyond the inlet throat. A horizontal cowl, having an height of 67 mm, is used. This simple geometry is able to generate an oblique shocks and a shock-train under the influence of the ramp and the cowl angles. The mentioned shock pattern can represent the flow distortions and the typical flow characteristics of a scramjet. The reference inlet condition of the test-case are:  $P_o = 10$  kPa,  $T_o = 300$  K and  $M_0 = 3$ .

We carried out the design of a single device combining the features of both the facility nozzle and of the inlet distortion generator. Several solutions have been found at different *in-flight* Mach numbers, as shown in Figure 4(a). The nozzle contours displayed in this plot have been computed by solving the inverse problem with backward MoC procedure. In general, the solution of the inverse problem by backward projection results in fast converging design, since the penalization of the objective function is avoided. Moreover, the two procedure do not lead to the same solution, as visible in Figure 4(b). The nozzle flowfield computed by the MoC procedure is reported in Figure 5. Only

## DESIGN OF INLET DISTORTION GENERATORS FOR SCRAMJET

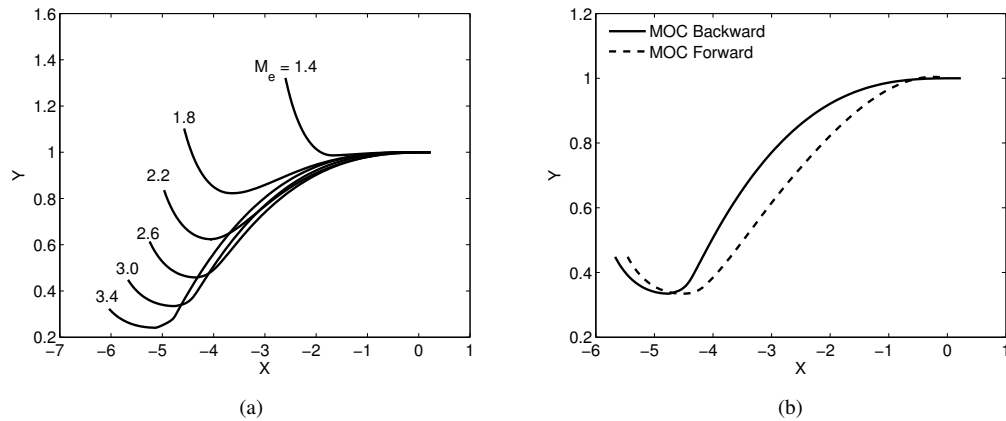


Figure 4: (a) Nozzle wall geometries at different *in-flight* Mach numbers  $M_0$ . (b) Comparison of nozzle geometry obtained by backward MoC and forward MoC procedures at  $M_0 = 3$ .



Figure 5: Mach number contourmap of the facility nozzle-IDG computed by MoC ( $M_0 = 3$ )

the supersonic portion of the flowfield is shown. The subsonic region of the nozzle is derived from the isentropic flow relations.

Both the free-jet configuration and the designed direct-connect rig are simulated and compared in Figure 6. The flow pattern generated by two designed direct-connect facility nozzle ( $M_0 = 2.2$  and  $M_0 = 3$ ) are checked against the corresponding flowfield of the scramjet model in in-flight conditions. The comparison has been performed by solving the Euler flow for the configurations here considered. A good agreement in the generated shock patterns can be appreciated in Figure 6 for both flight Mach numbers. The pressure distributions on the isolator upper surface are also well-matched in both conditions (Figure 7).

A set of CFD simulations based on the compressible URANS equations<sup>23,24</sup> are then carried out in order to assess the actual flow distortion at the cowl inlet. The computed Mach flowfield is depicted in Figure 8. As visible, the viscous effects and shock boundary layer interactions have a strong influence on the shock-train traveling towards the scramjet combustor. Without boundary layer bleed technologies, the flow exiting the facility nozzle is characterized by a viscous type velocity profile. The discrepancies between the velocity profile prescribed by the inviscid inverse procedure and the computed viscous solution are represented in the same figure. The inviscid solution slightly differs from the viscous in term of the reference Mach number. The error obviously increases close to the walls due to the different nature of boundary conditions in that region. Keeping in mind that we adopted an optimization tool based on genetic algorithms, the computationally lighter solution for this problem is the inclusion of loss/boundary layer models in the inverse procedure.

## Acknowledgements

Computational resources were provided by hpc@polito.it, a project of Academic Computing within the Department of Control and Computer Engineering at the Politecnico di Torino (<http://www.hpc.polito.it>).

## Conclusions

An hybrid approach to the aerodynamic design of a facility nozzle and as inlet distortion generator in a direct-connect scramjet combustor test-rig has been illustrated. As an initial assumption, it is required that the device should be able

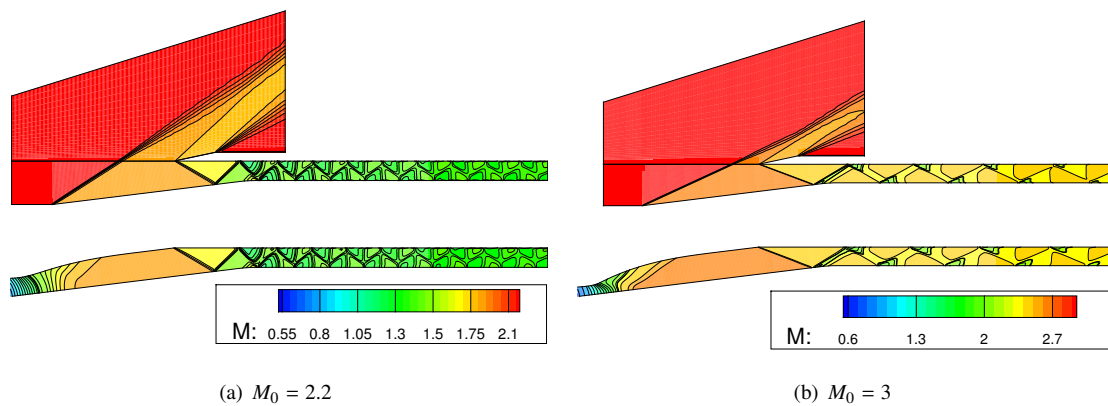


Figure 6: Mach isolines for the in-flight condition (*top*) and in the direct-connect facility (*bottom*)

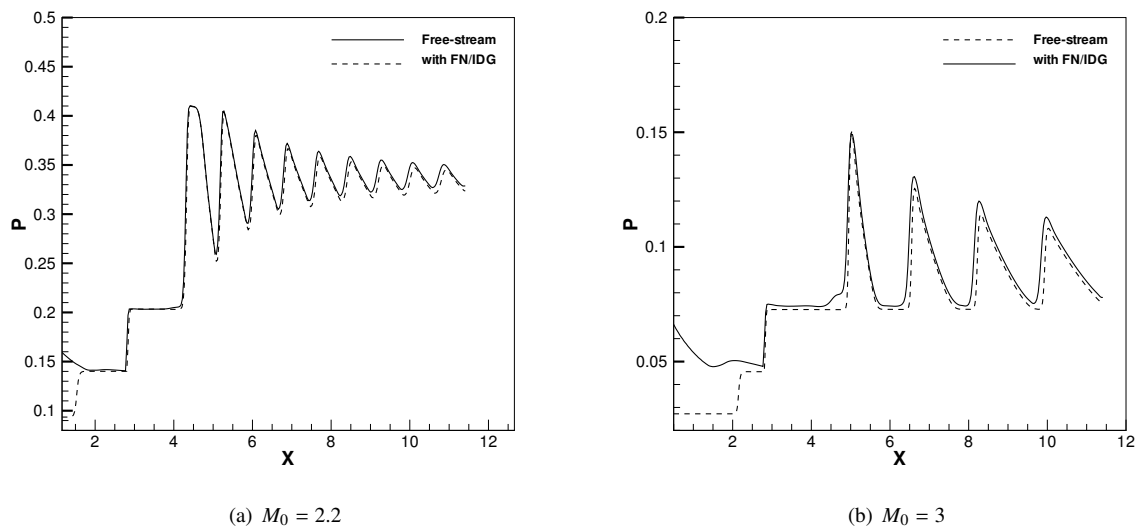


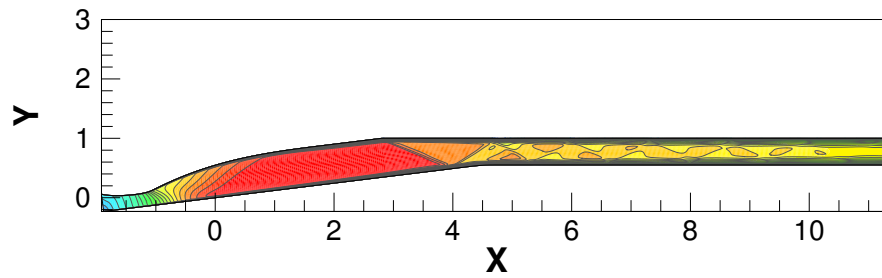
Figure 7: Comparison of the pressure distributions in the isolator upper-surface for the in-flight conditions and in the direct-connect facility

to replicate the reference operating point but also dynamic response of the system close to the operating point. This assumption restricts the choice of the reference section for the facility nozzle to inlet cowl section. The solution of the design problem was approached by using CFD and optimization tools having different levels of accuracy. Numerical tools based on the method of characteristics coupled to a GA optimizer have been employed in the design of the facility nozzle by solving an inverse problem. The CFD simulations carried out on the candidate solution have shown that the solutions found are able to reproduce the correct shock reflection pattern when compared to the corresponding in-flight configuration. The RANS computation on the same flowfields has good accuracy in the mean, but also put in evidence the need of some additional models to be included in the fast inverse solver in order to better match the physics of viscous flows, if the facility is not endowed with boundary layer bleed technologies.

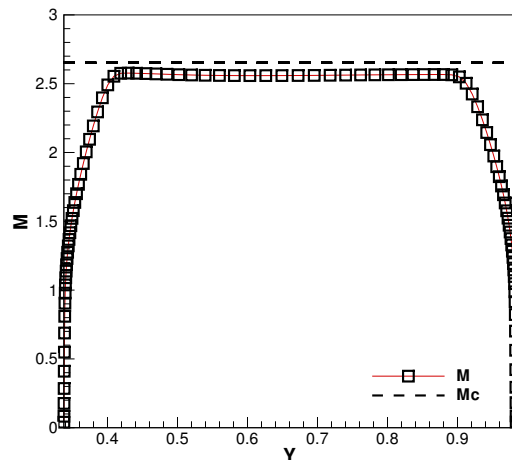
## References

- [1] S.C. Dunn. Ground testing techniques in support of flight test. *AIAA Paper 90-1309-CP, Orbital Debris Conference*, 1990.
- [2] R.R. Boyce, A. Paull, and R.J. Stalker. Unstarted inlet for direct-connect combustor experiments in a shock tunnel. *J. Propuls. Power*, 16(4):718–720, 2000.
- [3] C.J. Tam, K.Y. Hsu, M. Hagenmaier, and C. Raffoul. Simulations of inlet distortion effects in a direct-connect scramjet isolator. *AIAA Paper, 2011-5540*, 2011.
- [4] C.J. Tam and et al. Studies of inlet distortion in a direct-connect axisymmetric scramjet isolator. *Journal of Propulsion and Power*, 29(6):1382–1390, 2013.

## DESIGN OF INLET DISTORTION GENERATORS FOR SCRAMJET



(a)



(b)

Figure 8: RANS computation of the flowfield in the direct-connect facility, (a) Mach number contourmap, (b) velocity profile in front of the cowl inlet.

- [5] M.A. Hagenmaier, D.R. Eklund, and R.T. Milligan. Improved simulation of inflow distortion for direct-connect scramjet studies. *AIAA Paper*, 2011-233, 2011.
- [6] T. Mitani, N. Sakuranaka, S. Tomioka, and K. Kobayashi. Boundary-layer control in mach 4 and mach 6 scramjet engines. *Journal of Propulsion and Power*, 21(4):636–641, 2005.
- [7] M.R. Gruber, M.A. Hagenmaier, and T. Mathur. Simulating inlet distortion effects in a direct-connect scramjet combustor. *AIAA Paper*, 2006-4680, 2006.
- [8] K. Yu, J. Xu, L. Tang, and J. Mo. Inverse design of inlet distortion using method of characteristics for direct-connect scramjet studies. *Aerospace Science and Technology*, 46:351–359, 2015.
- [9] M. Ferlauto. An inverse method of designing the cooling passages of turbine blades based on the heat adjoint equation. *Proceedings of the Institution of Mechanical Engineers, Part A: Journal of Power and Energy*, 228(3):328–339, 2014.
- [10] P. Charbonneau. An introduction to genetic algorithms for numerical optimization. *NCAR Technical Note TN-450+IA*, 2002.
- [11] L.P. Riley, J. Hagenmaier, M.A. and Donbar, and D.V. Gaitonde. Isolator dynamics and heat release during unstart of a dual-mode scramjet. *55th AIAA Aerospace Sciences Meeting, AIAA SciTech Forum, AIAA paper 2017-0554*, 2017.
- [12] M. Ferlauto. A pseudo-compressibility method for solving inverse problems based on the 3D incompressible Euler equations. *Inverse Problems in Science and Engineering*, 23(5):798–817, 2015.
- [13] M.J. Zucrow and J.D. Hoffman. *Gas Dynamics, vols. 1, 2*. John Wiley and Sons, New York, 1976.
- [14] P.R. Spalart and S.R. Allmaras. A one-equation turbulence model for aerodynamic flows. *La Recherche Aérospatiale*, pages 5–21, 1994.
- [15] P.R. Spalart, F.T. Johnson, and S.R. Allmaras. Modifications and clarifications for the implementation of the spalart-allmaras turbulence model. *paper ICCFD7-1902, seventh International Conference on Computational Fluid Dynamics (ICCFD7), Big Island, Hawaii*, pages 1–11, 2012.

## DESIGN OF INLET DISTORTION GENERATORS FOR SCRAMJET

- [16] A. Harten, E. Engquist, and S. Osher. Uniformly high order accurate essentially non-oscillatory schemes. *Journal of Computational Physics*, 71:231–303, 1987.
- [17] M. Ferlauto and R. Marsilio. A computational approach to the simulation of controlled flows by synthetic jets actuators. *Advances in Aircraft and Spacecraft Science*, 2(1):77–94, 2014.
- [18] M. Ferlauto and R. Marsilio. A viscous inverse method for aerodynamic design. *Computer & Fluids*, 35(3):304–325, 2006.
- [19] C Ferrat and R. Marsilio. A computational method for combustion in high speed flows. *Computer & Fluids*, 70:44–52, 2012.
- [20] E.F. Toro. *Riemann Solvers and Numerical Methods for Fluid Dynamics. A Practical Introduction*. Springer-Verlag Berlin, 2009.
- [21] M. Pandolfi. A contribution to the numerical prediction of unsteady flows. *AIAA Journal*, 22:37–46, 1983.
- [22] T.J. Poinsot and S.K. Lele. Boundary conditions for direct simulations of compressible viscous reacting flows. *Journal of Computational Physics*, 101:104–129, 1992.
- [23] M. Ferlauto and R. Marsilio. A numerical method for the study of fluidic thrust vectoring. *Advances in Aircraft and Spacecraft Science*, 3(4):367–378, 2016.
- [24] M. Ferlauto and R. Marsilio. Numerical investigation of the dynamic characteristics of a dual-throat nozzle for fluidic thrust-vectoring. *AIAA Journal*, 55(1):86–98, 2017.